AUT Journal of Civil Engineering

AUT J. Civil Eng., 4(1) (2020) 91-102
DOI: 10.22060/ajce.2019.15195.5525

Finite difference method for buckling analysis of tapered Timoshenko beam made of functionally graded material

M. Soltani[1*], B. Asgarian[2], F. Jafarzadeh[3]

[1]Department of Civil Engineering, Faculty of Engineering, University of Kashan, Kashan, Iran
[2]Civil Engineering Faculty, K.N.Toosi university of Technology, Tehran, Iran
[3]Department of Civil Engineering, Faculty of Engineering, Shahr-e-Qods Branch, Islamic Azad University, Shahr-e-Qods, Iran

ABSTRACT: This paper addresses the linear buckling behavior of tapered Timoshenko beams made of axially functionally graded material (AFGM). Material properties of the non-prismatic Timoshenko beam vary continuously along the length of the member according to power law as well as exponential law. Based on Timoshenko beam assumption and using small displacements theory, the linear equilibrium equations are adopted from the energy principle for functionally graded non-uniform Timoshenko beams related to constant compressive axial load. The resulting system of stability equations are strongly coupled due to the presence of transverse deflection and angle of rotation. The differential equations are then uncoupled and lead to a single homogeneous differential equation where only bending rotation is present. The finite difference method (FDM) is then selected to numerically solve the resulting second-order differential equation with variable coefficients and determine the critical buckling loads. Two numerical examples are finally conducted to demonstrate the performance and efficiency of this mathematical procedure. The obtained results are contrasted with accessible numerical and analytical benchmarks.

Review History:
Received: 2018-10-31
Revised: 2019-02-21
Accepted: 2019-03-04
Available Online: 2019-03-04

Keywords:
Critical Buckling Load
Functionally Graded Material
Tapered Timoshenko Beam
Finite Difference Method

1-INTRODUCTION

Accurate evaluation of the critical buckling loads and stability limit state of elastic members is one of criteria in designing different structures. Euler-Bernoulli beam theory is commonly adopted for stability and free vibration analyses of long and slender beams with constant or variable cross-sections. According to this model, the effect of shear deformation is neglected and only the influence of flexural deformation is taken into consideration in the calculation process. Researchers usually use Timoshenko beam assumptions to model the behavior of short and thick beams such as towers, moveable arms and antenna, in which the influences of shear deformation and rotatory inertia are taken into account. Based on Timoshenko beam assumption and using small displacements theory, the stability behavior is governed by a pair of second order differential equations coupled in terms of the transverse deflection and the angle of rotation due to bending. In the last decades, with the development of manufacturing process, elastic members whose cross-sectional profile changes partially or gradually along their length, known as non-prismatic beams, have been widely spread in many engineering applications. This is because their ability in improving both strength and stability, satisfaction aesthetic necessities and optimization weight of structures. For Timoshenko beams with an arbitrarily variable cross-section, the stability analysis becomes more complex due to the presence of variable coefficients in the governing differential equations. Due to Timoshenko beam relevance to engineering configurations ranging from civil engineering to aeronautical applications, there are numerous researches dedicated to linear stability and vibration analyses of this member with constant or variable cross-section [1-11]. Despite these extensive studies for non-prismatic and prismatic elastic Timoshenko beams, the abovementioned researches are exclusively restricted to the buckling and dynamic analyses of homogeneous beam. By improvements in fabrication process, structural members are now adopted with different materials such as wood, steel and composite materials. Functionally Graded Materials (FGMs) as a new class of advanced materials are made up by gradually and smoothly changing the composition of two or more different materials in any desired direction. Engineers can thus produce structures with favorable stability and manage the distribution of material properties. Due to smooth variations in material properties, functionally graded materials can also overcome some disadvantages and weaknesses of laminated composites such as delamination and stress concentration. The use of non-prismatic beams made of functionally graded materials during the past twenty years has been increasing in complicated mechanical components such as turbine blades, rockets, aircraft wings and space structures due to their

*Corresponding author's email: msoltani@kashanu.ac.ir

conspicuous characteristics such as high strength, thermal resistance and optimal distribution of weight. Chakraborty et al. [12] introduced a new finite element solution based on the first-order shear deformation theory to investigate the thermo-elastic behavior of FG beam structures. Simsek and Kocatürk [13] investigated free vibration characteristics and the dynamic behavior of a simply-supported FG beam subjected to concentrated moving harmonic load. Further, Li et al. [14] has studied the free vibration behavior of axially inhomogeneous functionally graded beams by assuming material properties of the beam including Young's modulus and density to vary exponentially. Pradhan and Chakraverty [15] used Rayleigh–Ritz method to analyze the free vibration of Euler and Timoshenko functionally graded beams. Further, Arefi [16] investigated electromechanical stability of a functionally graded circular plate integrated with two functionally graded piezoelectric layers under radial compressive. By contemplating the impact of elastic foundation and semi-rigid end conditions, buckling analysis of axially functionally graded Euler-Bernoulli beam having non-uniform cross-section was surveyed in detail by Shvartsman and Majak [17]. Soltani [18] investigated free vibration behavior of axially functionally graded Timoshenko beams with varying cross-section through the power series method. Based on six different shear deformation theories, Pradhan and Chakraverty [19] surveyed free vibration behavior of functionally graded beam with various end restrains using Rayleigh–Ritz method. Based on the modified couple stress theory, mechanical behavior of non-uniform bi-directional functionally graded beam sensors was comprehensively studied by Khaniki and Rajasekaran [20]. Additionally, Li et al. [21] conducted instability analysis of a micro-scaled bi-directional functionally graded beam having rectangular cross-section by employing the Generalized Differential Quadrature Method (GDQM). Recently, Soltani and Asgarian [22] performed the stability analysis of cantilever axially functionally graded non-prismatic Timoshenko beam through a new finite element model based on power series approximation.

In previous authors' works [18, 22], the stability and free vibration analyses of axially functionally graded Timoshenko beam with varying cross-section has been investigated. For instance, a numerical technique based on the power series expansions of displacement components was utilized to simulate the problem [18], as well as finite element method [22]. The power series method [18] needs a considerable amount of time to determine explicit expressions of displacement functions for governing equilibrium equations. Another numerical method based on the power series expansions to acquire structural stiffness matrices was also proposed by authors to perform linear stability analysis of non-prismatic members with non-symmetric thin-walled cross-section [22]. However, this technique is only applicably for cantilever beams. The objective of the current paper is to present a new single governing equation in terms of angel of rotation for investigating the critical loads of axially functionally graded Timoshenko beam with non-uniform cross-section. Considering Timoshenko beam assumption and the effect of initial stress, the equilibrium equations and corresponding boundary conditions are established from the total potential energy of functionally graded non-uniform Timoshenko beams subjected to a constant compressive axial load tangential to the beam's axis. The governing equilibrium equations are derived in the case of elastic behavior and small displacements. The acquired system of linear stability equations are coupled in terms of the transverse deflection and the angle of rotation due to bending. The differential equations are then uncoupled and transformed to a single homogeneous differential equation where only bending rotation is present. Due to the complicated mathematical structure of the resulting differential equation, closed-form solutions are not accessible. In order to overcome this difficulty, the finite difference method (FDM) is utilized. Finite difference method, especially in its explicit formulation, is a very fast numerical method. Besides, it could be effectively tuned to achieve a desirable amount of accuracy. Regarding the finite difference rules, all the derivatives of the dependent variables in the resulting differential equation and the related boundary conditions are replaced with the corresponding forward, central and backward second order finite differences. Next, the discreet form of the governing equation is derived in a matrix formulation. The critical buckling loads are then determined by solving the eigenvalue problem of the obtained matrix. Finally, the effectiveness and reliability of this numerical technique in linear stability analysis have been confirmed by comparing the obtained numerical results with the outcomes of accessible numerical and analytical solutions for homogeneous and nonhomogeneous Timoshenko beams with variable cross-sections. The effects of material variations, taper ratios and end conditions on the critical buckling loads are also investigated intensively. It is worthy to note that these methodologies are employed to solve the linear stability problem for simply supported and clamped–free non-prismatic beams. Comments and conclusions are close to last section of present manuscript.

2-DERIVATION THE GOVERNING EQUATIONS

A non-prismatic Timoshenko beam of length $\boldsymbol{L}$ with axially variable material properties, as depicted in Fig.1, is taken into account. In this study, stability analysis is done considering small displacements. It is also contemplated that the beam is made from non-homogeneous material with shear (G) and Young's (E) moduli which are variable along the beam's length. A direct rectangular co-ordinate system is chosen, with x the initial longitudinal axis and y and z the first and second main bending axes, as depicted in Fig. 1. The origin of these axes is located at the centroid O. In the current research, the beam is undergoing a constant compressive axial load, which is tangential to the x-axis of member. Based on the Timoshenko beam theory, the longitudinal and transverse displacement components can be respectively expressed as:

$$U(x,y,z) = u_0(x) - z\,\theta(x)$$
$$W(x,y,z) = w(x) \qquad (1a, b)$$

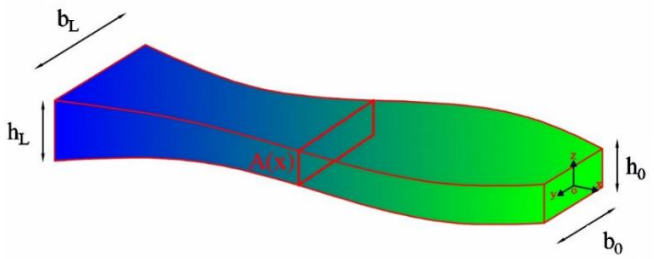

Fig. 1: An axially functionally graded Timoshenko beam with varying cross-section, Coordinate system and notation of displacement parameters

In the previous equations, U denotes the axial displacement, W signifies the vertical displacement (in z direction), and θ represents the angle of rotation of the cross-section due to bending. The equilibrium equations for non-prismatic Timoshenko beam are derived if the first variation of the total potential energy vanishes:

$$\delta\left(U+W_e\right)=0 \tag{2}$$

δ illustrates a virtual variation in the last formulation. $\boldsymbol{U}$ represents the strain energy and W_e denotes the work of applied loads. For the particular case of linear stability context, where the beam is not under any external forces, one considers that the external load work equals to zero. $\delta\,\boldsymbol{U}$ could be computed using the following equations:

$$\delta U=\int_L\int_A\left(\sigma_{xx}\,\delta\varepsilon_{xx}+\tau_{xz}\,\delta\gamma_{xz}\right)dA\,dx \tag{3}$$

In which, $\boldsymbol{L}$ and $\boldsymbol{A}$ express the element length and the cross-sectional area, respectively. $\delta\varepsilon_{xx}$ and $\delta\gamma_{xz}$ are strain tensor variations. σ_{xx} and τ_{xz} denote the Piola–Kirchhoff stress tensor components. Based on the assumption of the Green's strain-tensor, the strain-displacement relations and their first variation are:

$$\begin{aligned}&\varepsilon_{xx}=u_0{}'-z\theta'+\frac{1}{2}(w')^2\rightarrow\delta\varepsilon_{xx}=\\&\delta u_0{}'-z\delta\theta'+w'\delta w'\\&\gamma_{xz}=2\varepsilon_{xz}=w'-\theta\rightarrow\delta\gamma_{xz}=\delta w'-\delta\theta\end{aligned} \tag{4a, b}$$

Substituting Eq. (4) into Eq. (3), the expression of the virtual strain energy can be carried out as:

$$\delta U=\int_L\int_A\begin{pmatrix}\sigma_{xx}(\delta u_0{}'-z\delta\theta'+w'\delta w')+\\\tau_{xz}(\delta w'-\delta\theta)\end{pmatrix}dA\,dx \tag{5}$$

The variation of strain energy can be formulated in terms of section forces acting on cross-sectional contour of the elastic member in the buckled configuration. The section stress resultants are presented by the following expressions:

$$P=\int_A\sigma_{xx}\,dA$$

$$M=\int_A\sigma_{xx}\,z\,dA \tag{6a, c}$$

$$Q=\int_A\tau_{xz}\,dA$$

In which $\boldsymbol{N}$ is the axial force applied at end member. $\boldsymbol{M}$ and $\boldsymbol{Q}$ are respectively the bending moment and shear force at any point of the beam. Using relation (6), the final form of the strain energy variation (δU) is then acquired as:

$$\delta U=\int_L\begin{pmatrix}P(\delta u_0{}'+w'\delta w')+M\,\delta\theta'+\\Q(\delta w'-\delta\theta)\end{pmatrix}dx \tag{7}$$

According to the equation presented above, the first variation of strain energy contains the virtual displacements $(\delta u_0,\delta w,\delta\theta)$ and their derivatives. After appropriate integrations by parts, one gets an expression in terms of virtual displacements. After some calculations and needed simplifications, the following equilibrium equations in the stationary state are obtained:

$$\begin{aligned}&-P'=0\\&-(Pw')'-Q'=0\\&-M'-Q=0\end{aligned} \tag{8a, c}$$

The boundary conditions of the beam can be also expressed as:

$$\begin{aligned}&P=0 \quad Or \quad \delta\left(\partial u_0\right)=0\\&Pw'+Q=0 \quad Or \quad \delta\left(\partial w\right)=0\\&M=0 \quad Or \quad \delta\left(\partial\theta\right)=0\end{aligned} \tag{9a, c}$$

Assuming E and G to be the elastic parameters for an axially non-homogeneous material, which can be both variable through the longitudinal direction, the expression of the stress components including the normal and shear ones are as:

$$\sigma_{xx}=E(x)\varepsilon_{xx},\qquad\tau_{xz}=G(x)\gamma_{xz} \tag{10a, b}$$

Substituting the strain-displacement relations defined in Eq. (4) into elastic stresses of Eq. (10) and integration over the cross-sectional area in the context of principal axes, the following components are derived:

$$\begin{aligned}&P=\int_A\sigma_{xx}dA=\int_A E(x)\varepsilon_{xx}dA=\int_A E(x)\\&(u_0{}'-z\,\theta'+\frac{1}{2}(w')^2)dA=EA(u_0{}'+\frac{1}{2}(w')^2)\\&M=\int_A\sigma_{xx}\,z\,dA=\int_A E(x)\\&(u_0{}'-z\,\theta'+\frac{1}{2}(w')^2)z\,dA=EI\,\theta'\\&Q=\int_A\tau_{xz}\,dA=\int_A G(x)(w'-\theta)dA=kGA(w'-\theta)\end{aligned} \tag{11a, c}$$

In Eq. (12c), ***k*** is the shear correction factor. ***I*** denotes the minor moment of inertia about y-axis. In this study, it is assumed that the concentrated compressive axial load (***P***) is applied at end beam without any eccentricity (Fig. 1). This model is also established in the context of small displacements and deformations. According to linear stability, non-linear terms are also disregarded in the equilibrium equations. Based on these assumptions, the system of equilibrium equations for non–prismatic Timoshenko beam are finally derived by replacing Eq. (11) into Eq. (8):

$$\begin{aligned} &\left(EAu_0'\right)' = 0 \\ &\left(kGA\left(w'-\theta\right)\right)' - Pw'' = 0 \\ &(EI\theta')' + kGA\left(w'-\theta\right) = 0 \end{aligned} \qquad (12a, c)$$

In these differential equations, the successive x-derivatives are denoted by ( )', ( )". The last two equilibrium equations (12b and 12c) are coupled differential equations due to the presence of vertical and rotation displacement components (w and θ) and shear rigidity (GA). It is obvious that the equation for the axial displacement (Eq. (12a)) is uncoupled from the others and can be handled independently. The associated boundary conditions by ignoring the axial equation which has no incidence on stability analysis of Timoshenko beam are formulated as follows:

$$\begin{aligned} &\delta w: \quad kGA\left(w'-\theta\right) - Pw' = 0 \\ &\delta\theta: \quad EI\,\theta' = 0 \end{aligned} \qquad (13a, b)$$

The boundary condition in vertical direction (Eq. (13a)) can be transformed into:

$$w' = \left(\frac{kGA}{kGA-P}\right)\theta \qquad (14)$$

The last expression is incorporated in the third differential equation (Eq. (13c)). After some simplifications, Eq. (12c) is then uncoupled from the transverse displacement (w). The following differential equation is derived only in terms of the angle of rotation (θ):

$$(EI\theta')' + kGA\left(\left(\frac{kGA}{kGA-P}\text{-}1\right)\theta\right) = 0$$

Or

$$(EI\theta')' + kGA\left(\frac{P}{kGA-P}\theta\right) = 0 \qquad (15)$$

In order to solve the resulting second-order differential equation (Eq. (15)), prescribe boundary conditions including natural or geometrical ones at the two ends of the problem domain are required. It is noteworthy that the governing differential equation (Eq. (15)) is known as the strong form of the problem. Besides, to acquire the corresponding boundary conditions, the homogeneous differential equation should be transformed to a weighted-integral expression called the weak form which is equivalent to equilibrium equation and its relating boundary conditions. In order to construct the weak form for the governing differential equation, we should multiply Eq. (15) by an arbitrary function (ψ) and integrate the result over the problem domain. The weak form of the equilibrium equation in terms of bending rotation (Eq. (15)) is thus obtained by:

$$\int_0^L \psi\left((EI\theta')' + kGA\left(\frac{P}{kGA-P}\right)\theta\right)dx = 0 \qquad (16)$$

In which ψ is a test function which is continuous and satisfies the essential end conditions. Thus, the weak form for the equilibrium equation becomes:

$$\begin{aligned} &\int_0^L \left(-(EI\theta')\psi' + kGA\left(\frac{P}{kGA-P}\right)\theta\psi\right)dx + \\ &(EI\theta')\psi\Big|_0^L = 0 \end{aligned} \qquad (17)$$

In the current study, simply supported beams and cantilevers are surveyed. Their corresponding boundary conditions are thus obtained as follows:

Simply supported:

$$\theta'\big|_{x=0} = 0 \quad and \quad \theta'\big|_{x=L} = 0$$

Cantilever: (18a, b)

$$\theta\big|_{x=0} = 0 \quad and \quad \theta'\big|_{x=L} = 0$$

In order to simplify the solution procedure based on the considered numerical technique, the governing equilibrium equation is transformed to:

$$(kGA)(EI\theta')' + P\left(kGA\,\theta - (EI\theta')'\right) = 0 \qquad (19)$$

Extending the above equation results in:

$$\begin{aligned} &(kGA)\left(IE' + EI'\right)\theta' + (kGA)\left(EI\right)\theta'' + \\ &P(kGA)\theta - P\left(IE' + EI'\right)\theta' - P\left(EI\right)\theta'' = 0 \end{aligned} \qquad (20)$$

In the following section, the application of FDM in linear stability analysis of non-homogeneous Timoshenko beams with variable cross-section is presented.

3- FDM FORMULATION OF THE PROBLEM

As it was previously mentioned, closed-form solutions of the equilibrium equation due to the variable terms viz: cross-sectional area, moment of inertia and material properties are generally difficult. Therefore, an appropriate mathematical or numerical method must be adopted. Finite difference approach is a numerical iterative procedure that involves the use of successive approximations to obtain solutions of differential equations especially with variable coefficients. This approach is also capable of predicting the critical buckling loads with the desired precision. In order to apply the finite difference method to the equilibrium equation, the beam member with length of L is assumed to be sub-divided into n parts, with

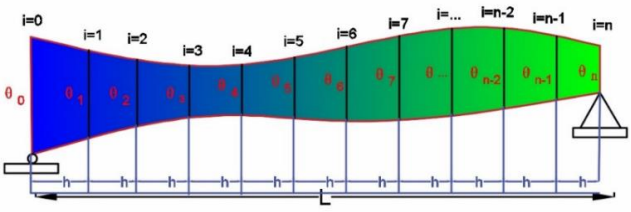

Fig. 2: Finite difference method: Definition spaced grid points

length ***h=L/n***, as shown in Fig. 2. Therefore, there are (n+1) nodes along the beam's length with number i=0,1…n, with 0 and n denote beam ends. From numerical point of view, the second order forward difference formulation is used for the first–node (i= 0) whereas for the last (i= n), the second order backward formulation is applied to the governing equation. For all the other nodes (0 <i < n), the second order central difference formulation is implemented.

According to central finite difference method, the first and second order derivatives of cross-section rotation angle ($\boldsymbol{\theta}$) for a discrete member are formulated as follows:

$$\theta_i' = \frac{\theta_{i+1} - \theta_{i-1}}{2h}$$

$$\theta_i'' = \frac{\theta_{i+1} - 2\theta_i + \theta_{i-1}}{h^2} \qquad \text{(21a, b)}$$

In which: θ_{i-1} θ_i and θ_{i+1} are angle of rotation of considered member in three points, located at equal distances of ***h***. By replacing the above formulations (Eq. (21)) in equation (19), and simplifications, the finite difference form of the governing differential equation at node i, can be expressed as follows:

$$\begin{aligned}
&h(kG_iA_i)(I_iE_i')(\theta_{i+1} - \theta_{i-1}) + \\
&h(kG_iA_i)(E_iI_i')(\theta_{i+1} - \theta_{i-1}) + \\
&2(kG_iA_i)(E_iI_i)(\theta_{i+1} - 2\theta_i + \theta_{i-1}) \\
&+2h^2P(kG_iA_i)\theta_i - Ph(I_iE_i') \\
&(\theta_{i+1} - \theta_{i-1}) - Ph(E_iI_i')(\theta_{i+1} - \theta_{i-1}) - \\
&2P(E_iI_i)(\theta_{i+1} - 2\theta_i + \theta_{i-1}) = 0
\end{aligned} \qquad \text{(22a)}$$

Or

$$\begin{aligned}
&(-kG_iA_i)(hI_iE_i' + hE_iI_i' - 2E_iI_i)\theta_{i-1} + \\
&(-4kG_iA_iE_iI_i)\theta_i + (kG_iA_i) \\
&(hI_iE_i' + hE_iI_i' + 2E_iI_i)\theta_{i+1} \\
&+P(hI_iE_i' + hE_iI_i' - 2E_iI_i)\theta_{i-1} + \\
&P(2h^2kG_iA_i + 4E_iI_i)\theta_i - \\
&P(hI_iE_i' + hE_iI_i' + 2E_iI_i)\theta_{i+1} = 0
\end{aligned} \qquad \text{(22b)}$$

Equation (22b) should be written for n-1 grid points of a divided element. (n-1) equations are thus derived including n+1 unknown parameters ($\theta_0, \theta_1, ..., \theta_n$). In order to solve the system of obtained equations by the finite difference method, two equations eventuated from boundary conditions of the beam are required as:

Pinned-Pinned:

$$\begin{cases} i = 0 \rightarrow -3\theta_0 + 4\theta_1 - \theta_2 = 0 \\ i = n \rightarrow 3\theta_n - 4\theta_{n-1} + \theta_{n-2} = 0 \end{cases} \qquad \text{(23a)}$$

Fixed-Free:

$$\begin{cases} i = 0 \rightarrow \theta_0 = 0 \\ i = n \rightarrow 3\theta_n - 4\theta_{n-1} + \theta_{n-2} = 0 \end{cases} \qquad \text{(23b)}$$

It is worth mentioning that forward and backward finite difference formulations are respectively implemented for the first (i=0) and last (i=n) nodes. In this manner, any virtual nodes are not required and the overall error is thus reduced. Therefore, finite difference approach in the presence of n equal segments constitutes a system of simultaneous equations with (n+1) linear equations. In the following, the simplified equilibrium equation through FD formulation is written in a matrix notation as follows:

$$([K] + P[K_G])\{\theta\}_{n+1\times 1} = \{0\}_{n+1\times 1} \qquad \text{(24)}$$

K and K_G are $n+1 \times n+1$ matrices. As mentioned previously, n denotes the number of segments along the computation domain ($0 \le x \le L$). Regarding Eq. (22b), the terms of K and K_G for $1 \le i \le n-1$ are determined in the following forms:

$$\begin{aligned}
&K_{i,i} = -kG_iA_i(hI_iE_i' + hE_iI_i' - 2E_iI_i); \\
&K_{i,i+1} = -4kG_iA_iE_iI_i; \\
&K_{i,i+2} = kG_iA_i(hI_iE_i' + hE_iI_i' + 2E_iI_i) \\
&K_{G_{i,i}} = hI_iE_i' + hE_iI_i' - 2E_iI_i; \\
&K_{G_{i,i+1}} = 2h^2kG_iA_i + 4E_iI_i; \\
&K_{G_{i,i+2}} = -(hI_iE_i' + hE_iI_i' + 2E_iI_i)
\end{aligned} \qquad \text{(25)}$$

in which, ***h*** is the length of each segment. In Eq. (24), {θ} is the displacement vector:

$$\{\theta\}^T = \{\theta_0 \quad \theta_1 \quad \theta_2 \quad \theta_3 \quad . \quad . \quad . \quad \theta_{n-2} \quad \theta_{n-1} \quad \theta_n\} \qquad \text{(26)}$$

The rest of constants in matrix [K] are obtained from the boundary conditions:

Pinned-Pinned:

$$\begin{cases} K_{n,1} = -3;\ K_{n,2} = 4;\ K_{n,3} = -1 \\ K_{n+1,n+1} = 3;\ K_{n+1,n} = -4;\ K_{n+1,n-1} = 1 \end{cases} \qquad \text{(27a)}$$

Fixed-Free:

$$\begin{cases} K_{n,1} = 1 \\ K_{n+1,n+1} = 3;\ K_{n+1,n} = -4;\ K_{n+1,n-1} = 1 \end{cases} \qquad \text{(27b)}$$

After wards, the critical buckling loads for Timoshenko beam with different boundary conditions (fixed–free and hinged–hinged) can be computed from the eigenvalues of Eq. (24). Note that all of the terms presented in the coefficient matrices ([K] and [K_G]) are real. Besides, [K] and [K_G]

are invertible matrices. It should be emphasized that the calculated axial critical loads are considered as real values.

4- NUMERICAL EXAMPLES:

In the previous sections, the equilibrium equation of axially functionally graded Timoshenko beam with varying cross-section was formulated and numerically solved for linear stability analysis. In this section, to study the effect of tapering ratio and material gradient on the critical load, two numerical examples relating to homogeneous and non-homogeneous Timoshenko beams with varying cross-section are included. In the following, the mechanical properties at the left support ($x=0$) and the right one ($x=L$) of the beam are respectively indicated with the subscripts 0 and 1. In order to simplify the solution procedure and the illustration of obtained results, two non-dimensional parameters are also adopted as:

$$r = I_0/(A_0 L^2) \qquad P_{nor} = P_{cr} L^2 / E_0 I_0 \tag{28a, b}$$

Where

$I_0 = h_0 b_0^3/12$ and $A_0 = b_0 h_0$.

The cross-section of all considered beams is in the form of rectangle with width h and depth b which is assumed to be sufficiently small relative to the width. It should be noted that Poisson's ratio and the shear correction factor in all presented cases are assumed to be 0.3 and 5/6, respectively.

In the first case (**Case A**), the height of the beam's section is (b_0) at the left support and linearly decreased to ($b_1 = (1-\beta)b_0$) at the other end. The width of the beam (h_0) remains constant. Therefore, the acquired section at the left end becomes a rectangle with a height of (b_1) and width of (h_0).

In **Case B**, the height and breadth of the beam are concurrently allowed to vary linearly along the member's length with sametapering ratio (β) to $b_1 = (1-\beta)b_0$ and $h_1 = (1-\beta)h_0$, respectively.

In this study, the tapering parameter (β) can change from zero (prismatic beam) to a range of [0.1, 0.9] for non-uniform beams. For the above-mentioned cases, the minor axis moment of inertia and the cross-section area can be respectively represented in the following forms:

Case A:

$$I = I_0 (1 - \beta x / L)^3 ; A = A_0 (1 - \beta x / L)$$

Case B: (29a, b)

$$I = I_0 (1 - \beta x / L)^4 ; A = A_0 (1 - \beta x / L)^2$$

4-1- Example 1- Tapered Timoshenko beam with power-law distribution of material properties:

As mentioned before, it is assumed that the considered FG beam in this research is composed of two different components and for such a member it can also becontemplated that the Young's modulus of elasticity varies continuously in the longitudinal direction according to a simple power-law function (P-FGM) of the volume fractions of the constituent materials while the Poisson's ratio is supposed to equal 0.3 along the beam axis:

$$E(x) = E_0 + (E_1 - E_0)(x / L)^m \tag{30}$$

E_0 and E_1 represent values of Young's modulus of the constituent materials. Note that E_0 is root elastic modulus. ***m*** signifies the material non-homogeneity index indicating the material variation profile through the length of the beam. It is supposed that tapered Timoshenko beam is made of a mixture of ceramic phase and metal phase. Regarding this, two different materials specifically Zirconia (ZrO_2) and Aluminum (***Al***) with the following characteristics are considered as: ZrO_2: E_0=200GPa; Al: E_1=70GPa.

According to the material property variation (Eq. (30)), the left side of AFG beam ($x=0$) is intended pure ceramic (Zirconia) and the right end ($x=L$) is pure metal (Aluminum). By notifying Eq. (30), it can also be concluded that by raising the power-law index (***m***), the proportion of zirconia over the beam's length increases. The linear stability analysis of the contemplated beams with varying rectangular cross-section has been performed using power-law index in the range of $0.3 \le m \le 3$.

The aim of the first section of this example is to define the required number of divisions in the longitudinal direction while using FDM to obtain an acceptable accuracy on critical elastic buckling loads. Regarding this, the lowest value of non-dimensional buckling load of the tapered beam related to Case ***A***, having various values of tapering ratios (β = 0.2, 0.5 and 0.8) and for two different boundary conditions are calculated with respect to the number of segments considered in the finite difference method. The convergence study is conducted out for AFG beam with non-homogeneity index of m=2. Note that the cross-sectional dimensions are taken by setting $r=0.01$ (Eq. (28a)). Besides, the elapsed time to perform numerical computations is displayed in this table. The calculated results are verified with the results obtained by finite element technique proposed by Shahba et al. [23] in Table 1. According to Table 1, it can be easily observed that an increase in the number of segments has a great effect on the convergence rate of critical load parameters at each case. This table shows that Central Processing Unit (CPU) needs an average of 14.67 seconds to accomplish finite difference method simulation for a pinned-pinned AFG tapered beam (α=0.5) with the number divisions equals to 40. The normalized buckling load is 2.0481 (error Δ=1.01%). In order to improve the results, more CPU times are needed. With 60 segments, the buckling parameter is 2.0353 (error Δ =0.37%) the CPU time is impressive (40.16 s). Finally, it can be concluded that that fifty number of segments (N=50) are sufficient to obtain the first buckling load parameters for different tapering ratios with desired accuracy.

Following the above mentioned procedure, the first non-dimensional buckling load parameter for various tapering ratios (β) with different gradient parameters (m=1, 2 and 3) are tabulated in Table 2. The outcomes related to beams made of homogenous material are also arranged in Table 2. It should be noted that the values of tapering ratio (β) are selected in such a way that make comparison possible with

Table 1: Effect of number of segments on the lowest non-dimensional critical buckling load parameters (P_{nor}) of FG tapered Timoshenko beam with two different end conditions and CPU time comparisons

Case	End Conditions	(⌧	The lowest non-dimensional critical buckling load						
			Number of Divisions						Shahba et al. [23]
			10	20	30	40	50	60	
A	Hinged-Hinged	0.2	4.2744 (2.10s)	4.1007 (5.04s)	4.0572 (9.54s)	4.0398 (16.17s)	4.0311 (24.23s)	4.0261 (38.37s)	4.0176
		0.5	2.2575 (2.40s)	2.1043 (5.18s)	2.0643 (9.34s)	2.0481 (14.67s)	2.0399 (24.65s)	2.0353 (40.16s)	2.0276
		0.8	0.7438 (2.66s)	0.6206 (6.15s)	0.5858 (12.97s)	0.5708 (22.35s)	0.5629 (45.28s)	0.5583 (53.25s)	0.5502
	Fixed-Free	0.2	1.6681 (2.34s)	1.6129 (6.77s)	1.5998 (12.25s)	1.5946 (24.35s)	1.5920 (38.70s)	1.5905 (56.85s)	1.5875
		0.5	1.0770 (2.68s)	1.0134 (6.96s)	0.9978 (12.41s)	0.9916 (25.71s)	0.9885 (40.47s)	0.9867 (57.11s)	0.9833
		0.8	0.4811 (2.72s)	0.4082 (7.05s)	0.3882 (12.50s)	0.3796 (25.82s)	0.3752 (41.94)	0.3725 (57.34s)	0.3676

Table 2: Non-dimensional buckling load parameter (P_{nor}) for axially FG tapered Timoshenko beam with different material non-homogeneity indexes (m) as well as homogeneous beam.

Material	Tapering ratio β	Case A				Case B			
		Hinged-Hinged	Fixed-Free			Hinged-Hinged	Fixed-Free		
		FDM	FDM	Soltani and Asgarian [22]	Δ(%)	FDM	FDM	Soltani and Asgarian [22]	Δ(%)
m=1	0.0	4.6673	1.7122	1.7101	0.123	4.66731	1.7122	1.7101	0.123
	0.2	3.3741	1.3599	1.3574	0.184	2.9257	1.2352	1.2326	0.211
	0.4	2.2196	1.0075	1.0043	0.319	1.5840	0.7913	0.7879	0.432
	0.6	1.2394	0.6571	0.6524	0.720	0.6634	0.4038	0.3991	1.178
	0.8	0.4786	0.3150	0.3076	2.406	0.1535	0.1170	0.1189	1.598
m=2	0.0	5.5558	1.9859	1.9815	0.222	5.5558	1.9859	1.9815	0.222
	0.2	4.0310	1.5920	1.5868	0.328	3.4868	1.4501	1.4446	0.381
	0.4	2.6564	1.1914	1.1855	0.498	1.8819	0.9392	0.9328	0.686
	0.6	1.4797	0.7840	0.7766	0.953	0.7802	0.4810	0.4730	1.691
	0.8	0.5629	0.3752	0.3655	2.654	0.1759	0.1364	0.1305	4.521
m=3	0.0	6.0492	2.1044	2.0966	0.372	6.0747	2.1044	2.0966	0.372
	0.2	4.4340	1.6999	1.6919	0.473	3.8388	1.5533	1.5451	0.531
	0.4	2.9396	1.2850	1.2764	0.674	2.0824	1.0198	1.0106	0.910
	0.6	1.6461	0.8568	0.8465	1.217	0.8649	0.5300	0.5185	2.218
	0.8	0.6266	0.4158	0.4028	3.227	0.1937	0.1509	0.1431	5.451
Homogenous	0.0	4.546	2.291	2.291	0.000	4.546	2.291	2.291	0.000
	0.2	5.674	1.884	1.884	0.000	5.036	1.743	1.742	0.057
	0.4	3.916	1.467	1.465	0.137	2.928	1.205	1.203	0.166
	0.6	2.332	1.032	1.029	0.292	1.337	0.691	0.688	0.436
	0.8	0.998	0.568	0.560	1.429	0.350	0.241	0.236	2.119

other available reference in the case of tapered Timoshenko beam made of axially functionally graded materials [22]. Besides, the relative errors between the finite element solution suggested by Soltani and Asgarian [22] for cantilever members and the proposed methodology are arranged in the mentioned table. As presented in Table 2, an outstanding compatibility between the critical buckling loads for different values of non-uniformity ratios acquired by the current study and those computed by Soltani and Asgarian [22] is observed.

Comparing the results of uniform beam and those of tapered ones (Table 2), it can be culminated that the considered prismatic beam in this example has the highest critical buckling load and is also most stable. This can be explained by the fact that an increase in tapering ratio causes reduction in cross-sectional area and moment of inertia and consequently in the stiffness of the elastic member and as a result, a weaker and more unstable beam is acquired. By pondering Eq. (30), it can be stated that when non-homogeneity index is

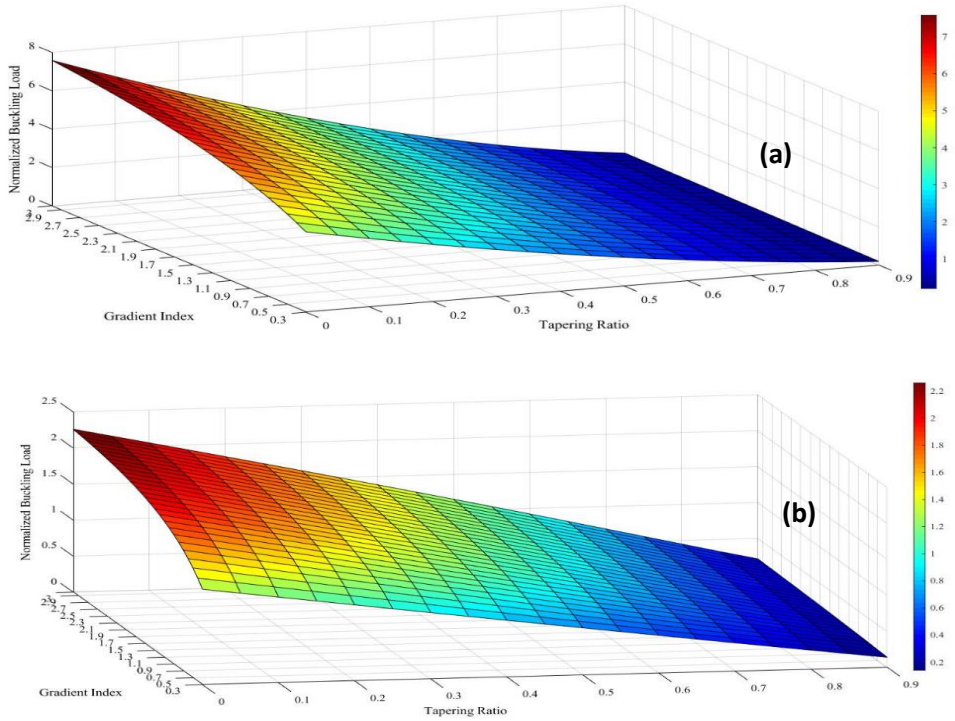

Fig. 3: Effects of the gradient index (*m*) on the normalized buckling load of double-tapered Timoshenko beam with different tapering ratios: (a) Simply supported (b) Cantilever

Table 3: The lowest normalized critical buckling load parameter (P_{nor}) for exponential FGM double tapered Timoshenko beam for various tapering ratios and two different end conditions

Tapering ratio (⊠)	Simply Supported				Fixed-Free			
	Gradient Parameter (⊠)				Gradient Parameter (⊠)			
	-1	-0.5	0.5	1	-1	-0.5	0.5	1
0.0	2.0422	2.9172	4.8096	5.5514	1.1122	1.4304	2.1587	2.5556
0.2	1.3179	1.9546	3.6757	4.5921	0.7828	1.0410	1.6704	2.0300
0.4	0.7378	1.1250	2.3712	3.2222	0.4861	0.6744	1.1779	1.4872
0.6	0.3222	0.5014	1.1584	1.6996	0.2385	0.3490	0.6881	0.9236
0.8	0.0792	0.1258	0.3105	0.4828	0.0636	0.1001	0.2360	0.3518

increased from 0.3 to 3, the volume fraction of Zirconia and consequently the value of Young's modulus are increased, and as a result, the beam becomes stiffer and more stable. In other words, a higher buckling load is achieved by an increase in the value of the gradient index (***m***).

Afterwards, the lowest buckling loads variation versus the tapering ratio (β) and the gradient index (***m***) for fixed-free and pinned-pinned double-tapered beams (Case B) is presented in Fig. 3. In the current section, the cross-sectional dimensions are taken by setting the aspect ratio (L/b_0) equals 5. As shown in Fig. 3, for any value of power-law exponent the stability of prismatic beam (β=0) and tapered beam with β=0.9 is most and least, respectively. It is also observed that for $0.3 \le m \le 1.2$, the non-dimensional critical loads relating to the first and second buckling modes increase sharply whereas, for $m > 1.2$, the buckling resistance increases slightly and approaches maximum magnitude.

4-2- Example 2- Double tapered Timoshenko beam with exponential distribution of material properties

In this example, linear stability analysis is accomplished for an exponential FGM Timoshenko beam having variable cross-section. In this regard, a double tapered beam with rectangular cross-section whose height and width taper linearly along the member axis is taken into account. Therefore, the cross-sectional area and moment of inertia are identical to Case ***B*** of the first example. In the current numerical example, the cross-sectional dimensions are taken by setting *r=0.05* (Eq. (28a)). The FG beam is assumed to be composed of ceramic and metal and for such a member it is also contemplated that the Young's modulus of elasticity vary continuously in the longitudinal direction according to an exponential function (E-FGM) of the volume fractions of the constituent materials while the Poisson's ratio is supposed to equal 0.3 along the beam axis:

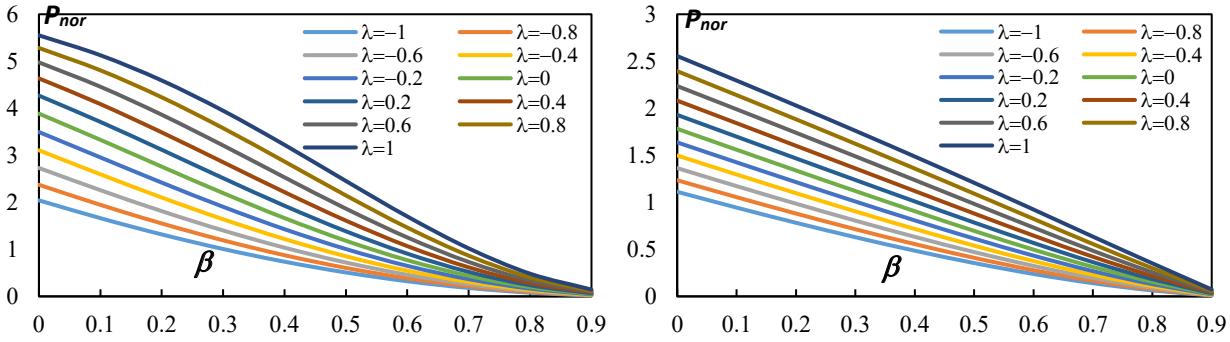

Fig. 4: Effects of the gradient parameter (*l*) on the normalized buckling load of double-tapered Timoshenko beam with different tapering ratios: (a) hinged-hinged (b) fixed-free.

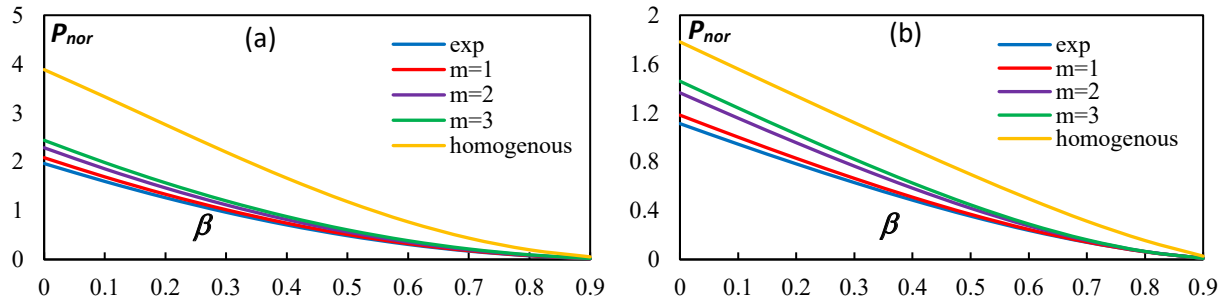

Fig. 5: Variation of dimensionless critical axial load with tapering parameter of ceramic-metal FG beam with Zirconia root for property distribution through the longitudinal direction as power law and exponential law as well as homogeneous beam: (a) Simply supported member, (b) Cantilever member.

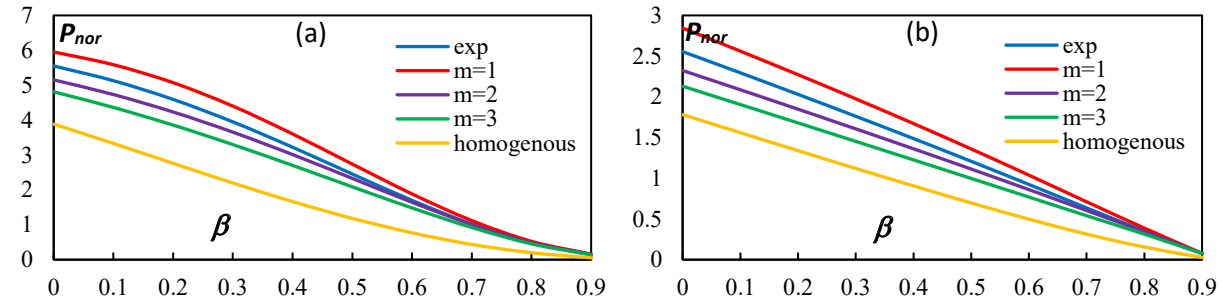

Fig. 6: Variation of dimensionless critical axial load with tapering parameter of metal-ceramic FG beam with Aluminum root for property distribution through the longitudinal direction as power law and exponential law as well as homogeneous beam: (a) Simply supported member, (b) Cantilever member.

$$E(x) = E_0 e^{\lambda \frac{x}{L}} \qquad \lambda = ln(E_1 / E_0) \tag{31}$$

E_0 and E_1 represent values of Young's modulus of the constituent materials. λ signifies a dimensionless parameter defining the gradual variation of the material property along the longitudinal direction. In the case of an isotropic and homogenous material λ equals zero. The above expression is adopted in several papers [14, 18, 20-22]. The lowest normalized buckling load parameters (P_{nor}) for different non-uniformity ratios (β) are arranged in Table 3. Moreover, Fig. 4 illustrates the variation of buckling loads of E-FG double tapered Timoshenko beam with respect to the taper ratio (β) and the gradient parameter (λ) for hinged-hinged and fixed-free members.

As can be seen in Fig. 4, the variation of stability behavior for the cantilever is similar to those for the hinged-hinged beam, but the latter beam is obviously more stable than the former. Moreover, for any value of gradient parameters the corresponding buckling load for the beam having constant cross-section is the highest and that for tapered beam with the tapering ratio (0.9) is the lowest. It is found from Fig. 4 that the variation of non-homogeneity parameter has a significant influence on the linear stability behavior of both beams under different circumstances. It can also be stated that the

critical buckling load parameters corresponding to the first mode are increased as the gradient parameter increases. The above-mentioned statement is reasonable due to the fact that Young's moduli rises as the value of inhomogeneous constant increases over zero $(\lambda>0)$, and the gradient parameter under zero$(\lambda<0)$ indicates Young's moduli decreases (see Eq. (31)).

In the following, comparison studies between the buckling resistance of ceramic-metal and metal-ceramic FG tapered Timoshenko beam having properties according to power law with different gradient indexes and exponential law are carried out and presented in Figs. 5 and 6. In this regard, we have determined the first non-dimensional buckling load with r=0.05 (Eq. (28a)) for double- tapered beams (Eq. (29b)) of hinged-hinged and fixed-free ends. Fig. 5 reveals the influence of tapering ratio (β) on the non-dimensional critical buckling load of ceramic-metal FG beam with Zirconia root and having properties according to power law with indexes m=1, 2 and 3 (Eq. (30)) as well as exponential law. The outcomes relating to homogenous beam are also plotted in this figure. In contrast with ***Al***, $\boldsymbol{ZrO_2}$ has superior mechanical properties. The material property distributions in AFG Timoshenko beam as power law with m=3 and exponential law makes the volume fraction of ceramic in the longitudinal direction of beam highest and lowest, respectively. Regarding this, the contemplated E-FGM beam has the lowest volume fraction of Zirconia and consequently, a weaker member compared to a beam having properties according to power law is achieved. Since the linear buckling resistance of beam is proportional to the stiffness of the members, it can be easily evident from this illustration that the buckling load corresponding to any value of tapering ratios is the lowest for beam with exponential volume fraction law and highest for the homogenous beam from ceramic (ZrO_2). Accordingly, the buckling load of beam having properties following simple power law with three different power law exponents (m=1, 2, 3) is between the above mentioned cases. In this case, the buckling resistance is higher for higher value of volume fraction indexes.

The variation of the lowest normalized buckling loads for metal-ceramic Timoshenko beams with aluminum root versus tapering parameters (β) are plotted in Fig. 6, for hinged-hinged and fixed-free beams having properties according to power law with indexes m=1, 2 and 3 (Eq. (30)) as well as exponential law (Eq. (31)). The non-dimensional buckling loads decrease substantially as the increase of non-uniformity constant $(\boldsymbol{\beta})$ for both type of property distribution similar to the results of beam with Zirconia root (Fig. 5). In contrast to ceramic-metal FG beam, the non-dimensional critical axial load of metal-ceramic member with aluminum root diminishes with increasing the power- law index (m) from 1 to 3. This phenomena can be explained by the fact that the percentage content of aluminum increases over the beam axis and this component has got lower shear and Young's modulus as compared to Zirconia and as a result weaker and more unstable beam is acquired. As is reflected in this figure, homogenous beam from Aluminum and FG beam having properties according to polynomial volume fraction law with m=1 have the normalized critical load with the smallest and largest values, respectively. Moreover, the presented outcomes also reveal that FG double-tapered Timoshenko beams with ***Al*** root and having properties according to power law with m=2, m=3 and exponential volume fraction law are intermediate stable.

5- CONCLUSIONS

In the present article, the finite difference method with second order accuracy is applied to investigate the critical buckling loads of non-prismatic axially functionally graded Timoshenko beams having two different end supports: hinged-hinged and clamped-free. In this regard, a new second order differential equation in terms of angle of rotation is obtained by uncoupling the system of differential equations governing the stability behavior of Timoshenko beam. The impact of width and/or height tapering ratios, axial variation of material properties and boundary conditions on linear buckling resistance of ceramic-metal and metal-ceramic Timoshenko beams are comprehensively surveyed. From the numerical examples, it could be concluded that by discretizing the considered member into 40-50 divisions the critical loads of AFG non-uniform members can be determined with a very good accuracy. It can be stated that the effects of width and/or height tapering ratios play important roles on the linear stability capacity of AFG tapered beam. It is also observed that, for ceramic-metal beams, buckling resistance increases with increase of functionally graded material content for both power-law (m) and exponential (λ) property distribution. In the case of ceramic-metal beam, it can be stated that FG beams having properties according to polynomial volume fraction law is more stable than beams having properties according to exponential law. Linear stability strength decreases with an increase of power law index for metal/ceramic beams with varying cross-section.

REFERENCES

1. Irie T., Yamada G., Takahashi I. (1980), "Vibration and stability of non-uniform Timoshenko beam subjected to a follower force", Journal of Sound and Vibration; 70: 503-512.
2. Lee S.Y, Lin S.M. (1995), "Vibrations of elastically restrained non-uniform Timoshenko beams", Journal of Sound and Vibration; 184(3): 403-415.
3. Esmailzadeh E., Ohadi A.R. (2000), "Vibration and stability analysis of non-uniform Timoshenko beams under axial and distributed tangential loads", Sound and Vibration; 236(3): 443-456.
4. Chen C.N. (2002), "DQEM vibration analysis of non-prismatic shear deformable beams resting on elastic foundations", Sound and Vibration; 255(5): 989-999.
5. Aucoello N.M., Ercolano A. (2002), "A general solution for dynamic response of axially loaded non-uniform Timoshenko beams", Solids and Structures; 41(18-19): 4861-4874.
6. Ruta P. (2006), "The application of Chebyshev Polynomials to the solution of the non-prismatic Timoshenko beam vibration problem", Sound and Vibration; 296(1-2): 243-263.
7. Wickowski Z., Colubiewski M. (2007), "Improvement in accuracy of the finite element method in analysis of stability of Euler-Bernouli and Timoshenko beam", Thin-walled Structures; 45: 950-954.
8. Ozdemir Ozgumus O., Kaya M.O. (2008), "Flapwise bending vibration analysis of a rotating double-tapered Timoshenko beam", Archive of Applied Mechanics; 78(5): 379-392.
9. Zhu B., Leung A.Y.T. (2009), "Linear and nonlinear vibration of non-uniform beams on two-parameter foundations using p-elements",

Computers and Geotechnics; 36: 743-750.
10. Soufyana A. (2009), "Exponential stability analysis of the linearized non-uniform Timoshenko beam". Nonlinear Analysis: Real world Application; 10: 1016-1025.
11. Attarnejad R., Shahba A., Jandaghi Semnani S. (2011), "Analysis of non-prismatic Timoshenko beams using basic displacement functions". Advances in Structural Engineering; 14(2): 319-332.
12. Chakraborty A., Gopalakrishnan S., Reddy J.N. (2003), "A new beam finite element for the analysis of functionally graded materials", International Journal Mechanical Science; 45: 519–39.
13. Simsek M., Kocatürk T. (2009), "Free and forced vibration of a functionally graded beam subjected to a concentrated moving harmonic load", Composite Structures; 90: 465–73.
14. Li X.F., Kang Y.A., Wu J. X. (2013), "Exact frequency equations of free vibration of exponentially graded beams", Applied Acoustic; 74: 413–420.
15. Pradhan K.K., Chakraverty S. (2013), "Free vibration of Euler and Timoshenko functionally graded beams by Rayleigh–Ritz method", Composite Part B; 51: 175–184.
16. Arefi M. (2015), "Nonlinear electromechanical stability of functionally graded circular plate integrated with functionally graded piezoelectric layers under radial compressive", Latin American Journal of Solids and Structures; 12(9): 1653-1665.
17. Shvartsman B., Majak J. (2016), "Numerical method for stability analysis of functionally graded beams on elastic foundation", Applied Mathematical Modelling; 44: 3713–3719.
18. Soltani M. (2017), "Vibration characteristics of axially loaded tapered Timoshenko beams made of functionally graded materials by the power series method", Numerical Methods in Civil Engineering; 2(1): 1-14.
19. Pradhan K. K., Chakraverty S. (2017), "Natural frequencies of shear deformed functionally graded beams using inverse trigonometric functions", Journal of the Brazilian Society of Mechanical Sciences and Engineering; 39(9): 3295-3313.
20. Khaniki H.B., Rajasekaran S. (2018), "Mechanical analysis of non-uniform bi-directional functionally graded intelligent micro-beams using modified couple stress theory", Materials Research Express; 5-055703.
21. Li X., Li L., Hu Y. (2018), "Instability of functionally graded micro-beams via micro-structure-dependent beam theory", Applied Mathematics and Mechanics (English Edition); 39: 923-952.
22. Soltani M., Asgarian B. (2019) "Finite element formulation for linear stability analysis of axially functionally graded non-prismatic Timoshenko beam". International Journal of Structural Stability and dynamics, 19(2): 1950002 (33 pages).
23. Shahb A., Attarnejad R., Tavanaie Marvi M., Hajilar S., (2011) "Free vibration and stability analysis of axially functionally graded tapered Timoshenko beams with classical and non-classical boundary conditions", Composites: Part B; 42(4): 801-808.

HOW TO CITE THIS ARTICLE

M. ESoltani, B. Asgarian, F. Jafarzadeh, Finite difference method for buckling analysis of tapered Timoshenko beam made of functionally graded material, AUT J. Civil Eng., 4(1) (2020) 91-102.

DOI: 10.22060/ajce.2019.15195.5525